PNAS
www.pnas.org

Supplementary Information for

Photosystem II oxygen-evolving complex photo-assembly displays an inverse H/D solvent isotope effect under chloride-limiting conditions

David J. Vinyard, Syed Lal Badshah, M. Rita Riggio, Divya Kaur, Annaliesa R. Fanguy, and M. R. Gunner

Corresponding author: David J. Vinyard
Email: dvinyard@lsu.edu

This PDF file includes:

www.pnas.org/cgi/doi/10.1073/pnas.1910231116

Supplemental Materials and Methods

PSII sample preparations

PSII membranes were isolated from market spinach using the "BBY" protocol (1) with minor modifications (2). All sample preparation and analysis steps were performed on ice in darkness with only dim green LED illumination. As measured immediately following isolation, these PSII membranes had O_2 evolution activities of 780-810 μmol O_2 (mg Chl)$^{-1}$ h^{-1}. Samples were stored at -80°C with 30% (v/v) ethylene glycol as a cryoprotectant (3).

To prepare samples for photo-assembly, approximately 50 mg Chl as PSII membranes were thawed and pooled. These samples were washed two times in 50 mM MES, pH 6.0, 10 mM $CaCl_2$, 15 mM NaCl, 400 mM sucrose, and 0.01% (v/v) Triton X-100. All washing steps involved centrifugation at 38,000 x g for 20 min and resuspension of the pellet using a soft brush followed by homogenization using a manual tissue grinder. At this stage, a fraction of the total sample was saved, labeled "Control PSII membranes," and stored at -80°C. Because of freeze/thaw cycles, handling, and the use of sucrose as a cryoprotectant, the activity of these control PSII membranes was approximately 400 μmol O_2 (mg Chl)$^{-1}$ h^{-1} (Table S1).

Next, extrinsic subunits were removed using a high divalent salt wash (4). The remaining sample from the step above was spun down and resuspended in 50 mM MES, pH 6.0, 1 M $CaCl_2$, and 400 mM sucrose to a final concentration of 0.5 mg Chl mL^{-1}. The sample was incubated on ice for one hour with periodic homogenization. The sample was then spun down, resuspended in the same buffer containing 1 M $CaCl_2$, homogenized, and immediately spun down again. This second wash step helped remove a larger fraction of PsbP and PsbO. The sample was washed three times in 50 mM MES, pH 6.0, 25 mM $CaCl_2$, 200 mM NaCl, 400 mM sucrose, and 0.01% (v/v) Triton X-100. These steps removed excess $CaCl_2$, but both [Ca^{2+}] and [Cl^-] were kept relatively high to maintain the OEC (5, 6). At this stage, a fraction of the total sample was saved, labeled "Extrinsics-depleted PSII membranes," and stored at -80°C.

The OEC was removed using the reducing agent hydroxylamine and the chelator EDTA. The remaining sample from the step above was spun down and resuspended in 50 mM MES, pH 6.0, 10 mM $CaCl_2$, 15 mM NaCl, 400 mM sucrose, 0.01% (v/v) Triton X-100, 5 mM EDTA, and 5 mM NH_2OH to a final concentration of 0.5 mg Chl mL^{-1}. This buffer was prepared immediately before use. The sample was incubated on ice for 10 min with periodic homogenization. The sample was then washed three times in 50 mM MES, pH 6.0, 10 mM $CaCl_2$, 15 mM NaCl, 400 mM sucrose, 1 mM EDTA, and 0.01% (v/v) Triton X-100, and two times in 25 mM MES, pH 6.0, and 400 mM sucrose. The final sample was labeled "apo-OEC PSII membranes" and stored at -80°C. Multiple small aliquots

were made so that all photo-assembly samples had the same history of freeze/thaw cycles.

PSII sample characterization

For all experiments in this work, PSII activity was measured as the rate of light-induced O_2 evolution measured using a Hansatech Oxygraph system. Saturating illumination was provided by a red LED (λ_{max} = 623 nm, ~4 W optical power). All O_2 assays were performed at 25°C in 25 mM MES, pH 6.0, 25 mM $CaCl_2$, 50 mM NaCl, 1 mM potassium ferricyanide, 0.25 mM phenyl-1,4-benzoquinone (recrystallized two times from ethanol), and 5-10 μg chlorophyll as PSII membranes.

For EPR quantification of Mn content, 0.15 mg chlorophyll as PSII membranes was digested in trace metal grade nitric acid (14 M final HNO_3). Samples were incubated in sealed plastic tubes for one day at room temperature before being centrifuged to remove any residual debris and transferred to quartz EPR tubes. EPR spectra were measured on a Bruker EMX spectrometer equipped with a standard cavity and an ESR900 helium flow cryostat. Multiple microwave powers were tested to ensure signals were not saturated. Experimental parameters were microwave frequency, 9.47 GHz; microwave power, 4 mW; modulation frequency, 100 kHz; modulation amplitude, 20 G; sweep time, 42 s; conversion time, 21 ms; time constant, 82 ms.

For protein subunit analysis, 3 μg chlorophyll as PSII membranes was denatured on ice for one hour using sample buffer containing 2% lithium dodecyl sulfate and 2% β-mercaptoethanol. SDS-PAGE was performed using a 12% polyacrylamide gel containing 6 M urea. Protein bands were visualized by silver staining. A second SDS-PAGE gel with the same loading was used for immunoblotting. A polyclonal rabbit α-PsbO antibody was a gift from Prof. Terry Bricker (Louisiana State University) and was used at a dilution of 1:20,000. Chemiluminescence was used to detect the signal from a commercial goat α-rabbit secondary antibody conjugated to horseradish peroxidase (Invitrogen). Densiometry was performed using ImageJ.

OEC photo-assembly

Thawed and homogenized apo-OEC PSII membranes were added to photo-assembly buffer and freshly prepared dichlorophenolindophenol (DCIP). All photo-assembly reactions contained 0.25 mg mL^{-1} chlorophyll as apo-OEC PSII membranes, 25 mM MES, 400 mM sucrose, 8 mM $NaHCO_3$, and 10 μM DCIP. $NaHCO_3$ was added because it has a positive effect on photo-assembly rates (7) and ensures that the PSII acceptor-side non-heme iron is not perturbed (8). Variable concentrations of $MnCl_2$, $CaCl_2$, and NaCl, and variable pH values (controlled by titrating MES free acid with NaOH) were used as described in Results.

For experiments using D_2O, buffers were prepared using fresh 99.9% D_2O. pD was calculated according to Glasoe and Long where $pD = pH_{reading} + 0.4$ (9). Upon diluting

apo-OEC PSII membrane samples (in H_2O) in photo-assembly buffer prepared in D_2O, the final D_2O concentration is estimated as 92%.

All photo-assembly reactions were prepared to a final volume of 150 µL in clear 1.5-mL microcentrifuge tubes. All preparation steps were performed in darkness using only dim green LED illumination. Photo-assembly was induced by transferring reactions to a 25°C incubator equipped with a nutating mixer and dimmable cool white light illumination. Average light intensity at the sample surface was measured using a LI-COR LI-250A light meter.

Following photo-assembly, samples were immediately placed on ice and maintained in darkness. 10 µg of chlorophyll from the photo-assembly reaction was removed to measure O_2 evolution rate. The time from the end of photo-assembly to the O_2 evolution measurement was less than 20 min for all samples. O_2 evolution rates were measured as described above. When photo-assembly was performed in D_2O, O_2 evolution rates were measured in H_2O.

Because the photo-assembled PSII samples do not contain extrinsic subunits, O_2 evolution rates were normalized to the rate of extrinsics-depleted PSII membranes under identical measurement conditions. This value is reported as photo-assembly yield.

Data analysis

All experiments were performed with 3-6 replicates. Means and standard errors are reported. Data were analyzed using Origin 2016.

Heat maps shown in Figure 2 and Figure S3 were generated in Origin 2016. First, a matrix of yield values was constructed. The range of 0 to the maximum element value was divided into eight major levels as indicated by black lines in each plot. Major levels were then divided into five minor levels. A color scale from blue (low) to red (high) was used illustrate relative values. Black dots represent the data points used to generate each plot.

To fit the sigmoidal curves from photo-assembly kinetic data, we used a similar strategy as that used to model bacterial growth curves using a modified Gompertz equation (10) (Equation 2).

$$\boldsymbol{y = A\, exp\left\{-exp\left[\frac{\mu \cdot e}{A}\left(T_{lag} - t\right) + 1\right]\right\}} \qquad [2]$$

In this model, µ is the absolute rate during the growth phase in (units s^{-1}), T_{lag} is the extent of the lag phase (units s), and A is the maximal yield reached at steady state. The

average rate of the lag phase, k_{lag}, was calculated as $1/T_{lag}$. μ is reported in Table 1 as k_{growth}.

MCCE Simulations

MCCE calculations were carried out on the complete apo-OEC PSII crystal structure PDB 5MX2 (11). In addition, MCCE calculations were performed for comparison by removing the OEC cluster from the QM/MM optimized S_1 sphere (12). The S_1 sphere structure includes the following residues: D1 (chain A): (57)-V58-V67-(68), (81)-V82-L91-(92), (107)-N108-Y112-(113), (155)-A156-I192-(193), (289)-I290-N298-(299), (323)-A324-A344:C-terminus; CP43 (chain C): (290)-W291-(292), (305)-G306-A314-(315), (334)-T335-L337-(338) ,(341)-M342-(343), (350)-F351-F358-(359), (398)-A399-G402-(403), (408)-G409-E413-(414); D2 (chain D): (311)-E312-L321-(322), (347)-R348-L352:C-terminus. Only backbone atoms are considered for capping residues indicated by parentheses. There are two crystallographic chloride ions in the structure: one of the chlorides is near D2-K317, while the other is near D1-N338 and D1-F339. These chlorides were either retained or removed as indicated.

The details of MCCE isosteric sampling are described in reference (13). The MCCE conformer sampling fixes the C, N, and O positions of the amino acid side chain while sampling the neutral and ionized protonation states of Glu, Asp, Arg, Lys, His and Tyr (13). In addition, tautomers of histidine are included while the hydroxyl protons are allowed to exchange in Asn and Gln terminal O and N positions. For the primary ligands, D1-D170, D1-E189, D1-E333, D1-D342, and CP43-E354, additional rotational degrees of freedom are included by sampling side chain rotamers (14).

All the crystallographic waters are removed from the structure and are replaced by implicit solvent with a dielectric constant of 80. The Delphi Poisson-Boltzmann electrostatics energies are computed using the dielectric constant for protein to be 4. Parse charges (15) are used for amino acid residues while standard MCCE topology files are used for chlorides. The calculations used implicit salt concentration of 0.15 M along with a 2 Å Stern layer. The pH varied from 5.5 to 7.0. Monte Carlo simulations are carried out to determine the Boltzmann distribution for all degrees of freedom, which yields the probability each ionizable residue being protonated.

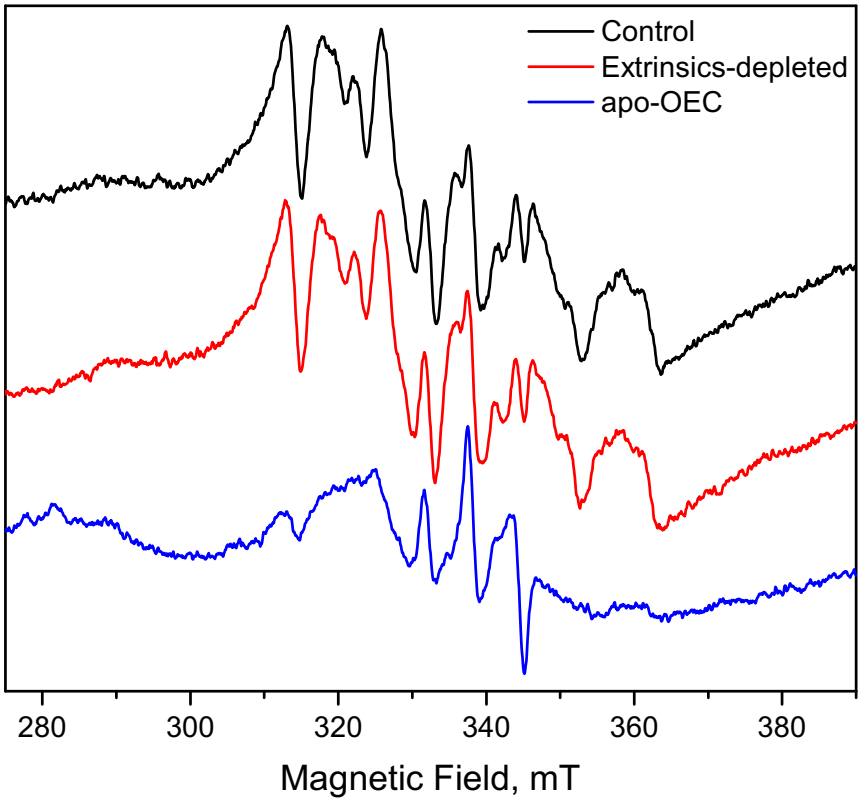

Figure S1. Mn quantification of nitric acid-digested PSII membrane samples. The six-line EPR signal from Mn^{2+} is of similar magnitude in the control and extrinsics-depleted samples. This signal is decreased by approximately 85% in the apo-OEC sample. Spectra were recorded at 9.47 GHz at 7.4 ± 0.1 K.

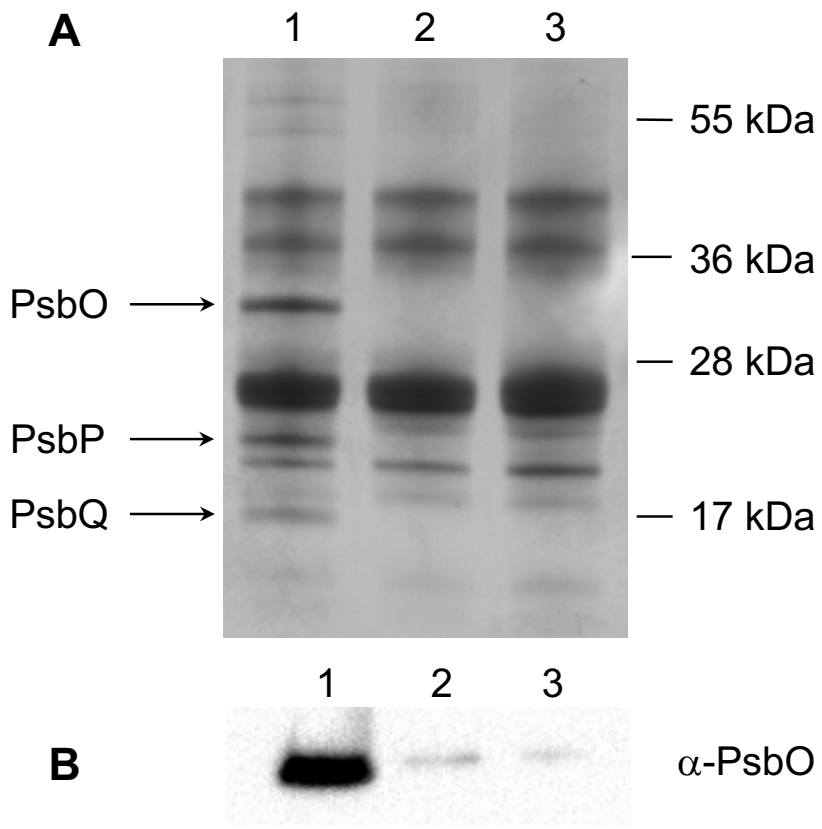

Figure S2. (A) Silver-stained SDS PAGE analysis and (B) α-PsbO immunoblot of PSII membrane samples. Lane 1 – control, Lane 2 – extrinsics-depleted, Lane 3 – apo-OEC. Densiometry analysis of the immunoblot shows that 92% of PsbO is removed in the extrinsics-depleted sample and 96% of PsbO is removed in the apo-OEC sample.

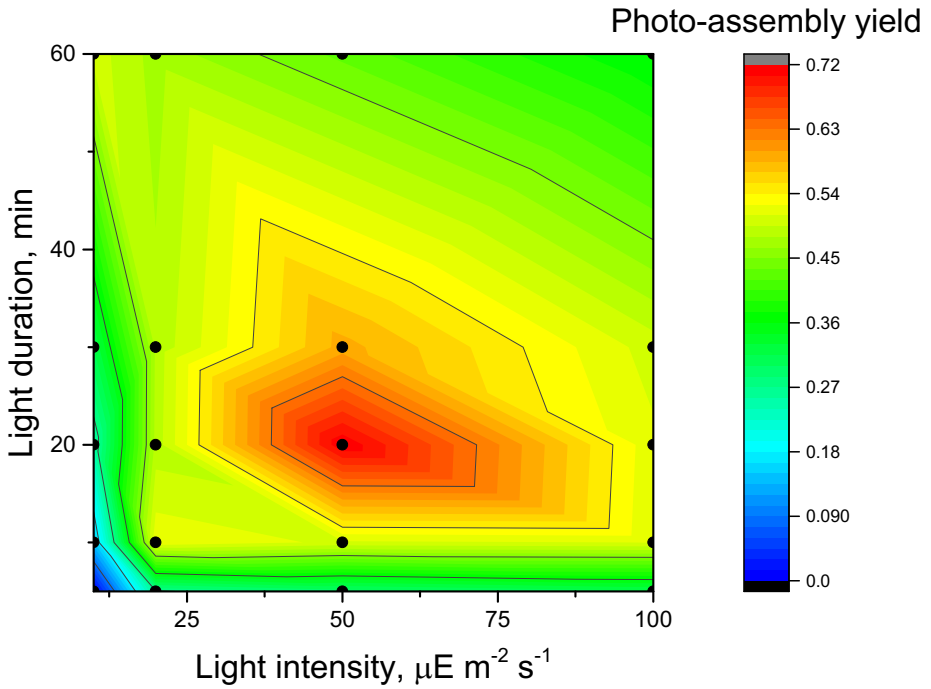

Figure S3. Two-dimensional optimization of photo-assembly light duration and light intensity. Samples contained 0.25 mM Mn^{2+}, 40 mM Ca^{2+}, 670 mM Cl^{-}, 8 mM HCO_3^{-}, 25 mM MES, pH 6.0, 400 mM sucrose, 10 μM DCIP, and 0.25 mg/mL chlorophyll as apo-OEC PSII membranes. Dots represent the 20 reactions used the generate the plot (light intensities of 10, 20, 50 and 100 μE m^{-2} s^{-1}, and light durations of 5, 10, 20, 30, and 60 min).

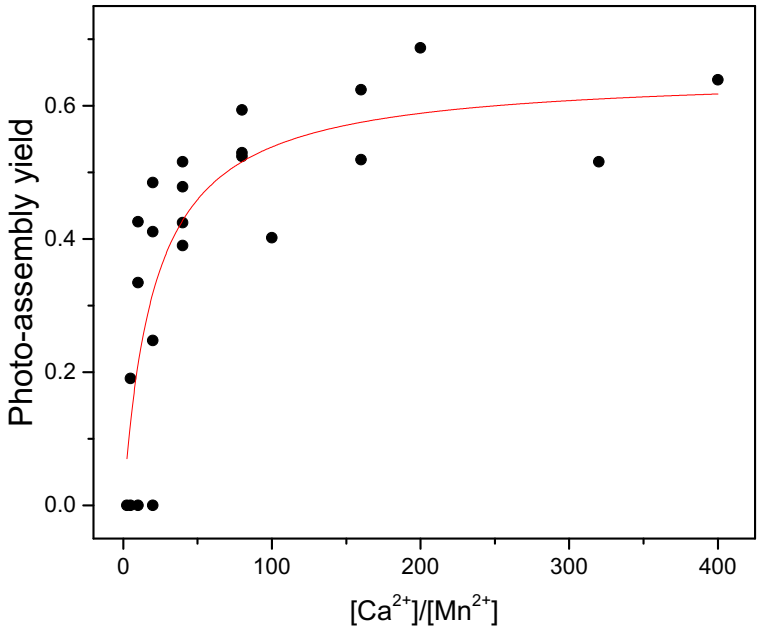

Figure S4. Photo-assembly yield depends on the ratio of Ca^{2+} to Mn^{2+}. Sample conditions were similar to those in Figure S3, but [Mn^{2+}] was varied from 0.1-2 mM and [Ca^{2+}] was varied from 5-80 mM. NaCl was varied to maintain constant [Cl^{-}]. All photo-assembly reactions were exposed to 50 µE m^{-2} s^{-1} for 20 min.

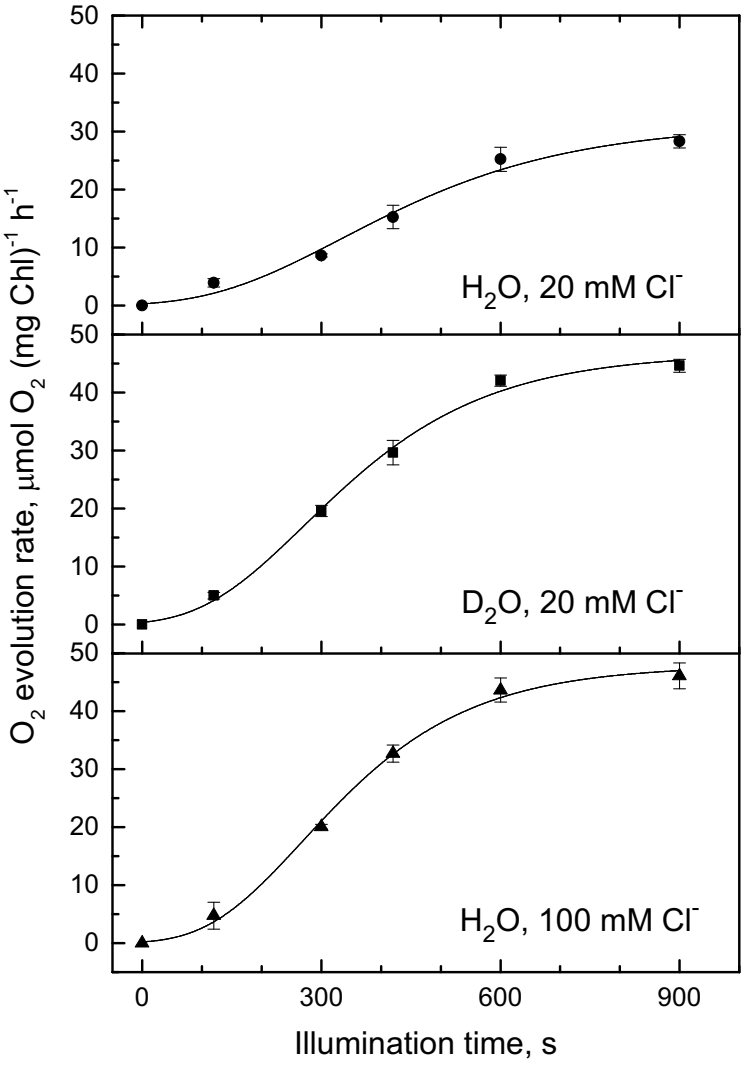

Figure S5. Rates of photo-assembly are dependent on solvent and chloride concentration in the presence of PsbO. PSII membranes used for this experiment were prepared as described in Supplemental Materials and Methods *except* 2 M NaCl was used to wash the membranes instead of 1 M $CaCl_2$. This treatment preserves binding of the PsbO subunit. Because the chloride dependence of photo-assembly is lower when PsbO is bound, low chloride samples were photo-assembled using 10 mM $CaCl_2$ and 0.1 mM $MnCl_2$ (20.2 mM total Cl^-, $[Ca^{2+}]$:$[Mn^{2+}]$ = 100). High chloride samples were photo-assembled using 40 mM $CaCl_2$, 20 mM NaCl, and 0.4 mM $MnCl_2$ (100.8 mM total Cl^-, $[Ca^{2+}]$:$[Mn^{2+}]$ = 100). Data with error bars represent average values and standard error (n = 3-4). Traces represent kinetic analyses described in Table S2.

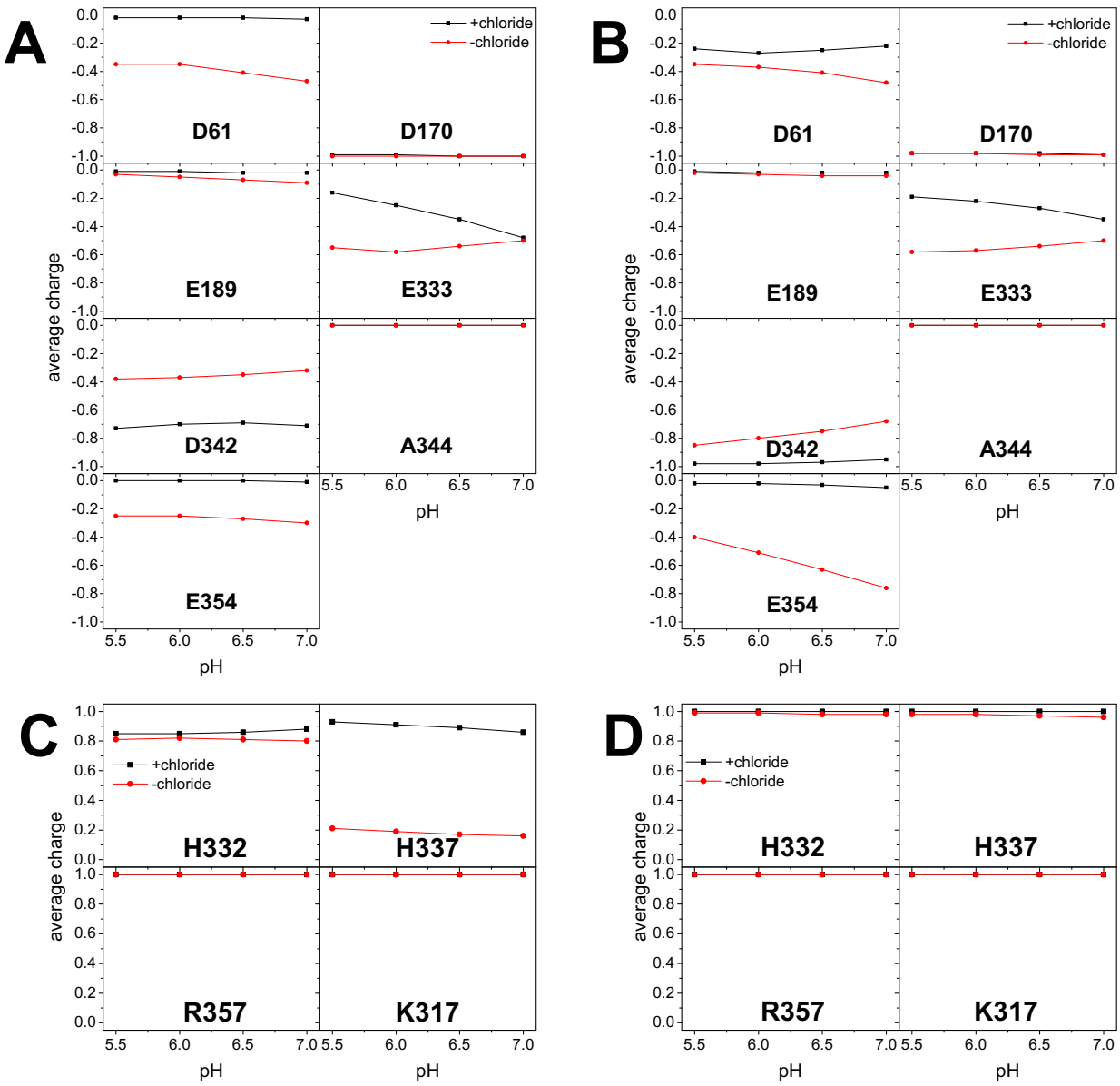

Figure S6. MCCE simulated charges of acidic (A and B) and basic (C and D) residues in and near the apo-OEC binding site based on either the 5MX2 (A and C) or cluster-depleted S_1 (B and D) structures. A3444 is the C-terminus of the D1 peptide. Black squares and lines represent simulations where chloride was added, and red circles represent simulations where chloride was removed.

Table S1. O_2 evolution rates of spinach PSII membrane samples. Samples were measured in a buffer containing 25 mM MES, pH 6.0, 25 mM $CaCl_2$, 50 mM NaCl, 1 mM potassium ferricyanide, 0.25 mM phenyl-1,4-benzoquinone.

Control PSII membranes	414 ± 11 µmol O_2 (mg Chl)$^{-1}$ h^{-1}
Extrinsics-depleted PSII membranes [a]	44.1 ± 0.9 µmol O_2 (mg Chl)$^{-1}$ h^{-1}
apo-OEC PSII membranes [b]	0.5 ± 2.7 µmol O_2 (mg Chl)$^{-1}$ h^{-1}

[a] 1 M $CaCl_2$ washed Control PSII membranes

[b] 5 mM NH_2OH and 5 mM EDTA washed apo-OEC PSII membranes

Table S2. Rates of photo-assembly in the presence of PsbO were determined by fitting data from Figure S4. Errors represent uncertainty of the fit.

solvent	[Cl^-], mM	*lag phase* duration, T_{lag}, s	*average lag phase rate,* k_{lag}, s^{-1}	*growth phase rate,* k_{growth}, s^{-1}
H_2O	20	117 ± 45	0.0085 ± 0.0033	0.053 ± 0.009
D_2O	20	99 ± 21	0.010 ± 0.002	0.099 ± 0.009
H_2O	100	110 ± 18	0.0090 ± 0.0014	0.111 ± 0.009

References

1. Berthold DA, Babcock GT, & Yocum CF (1981) A highly resolved, oxygen-evolving photosystem II preparation from spinach thylakoid membranes. *FEBS Lett.* 134(2):231-234.
2. Ghanotakis DF & Babcock GT (1983) Hydroxylamine as an inhibitor between Z and P680 in photosystem II. *FEBS Lett.* 153(1):231-234.
3. Beck WF, De Paula JC, & Brudvig GW (1986) Ammonia binds to the manganese site of the oxygen-evolving complex of photosystem II in the S_2 state. *J. Am. Chem. Soc.* 108(14):4018-4022.
4. Ono T-A & Inoue Y (1983) Mn-preserving extraction of 33-, 24- and 16-kDa proteins from O_2-evolving PS II particles by divalent salt-washing. *FEBS Lett.* 164(2):255-260.
5. Ghanotakis DF, Babcock GT, & Yocum CF (1984) Calcium reconstitutes high rates of oxygen evolution in polypeptide depleted Photosystem II preparations. *FEBS Lett.* 167(1):127-130.
6. Bricker TM (1992) Oxygen evolution in the absence of the 33-kilodalton manganese-stabilizing protein. *Biochemistry* 31(19):4623-4628.
7. Baranov SV*, et al.* (2004) Bicarbonate Is a Native Cofactor for Assembly of the Manganese Cluster of the Photosynthetic Water Oxidizing Complex. Kinetics of Reconstitution of O_2 Evolution by Photoactivation. *Biochemistry* 43(7):2070-2079.
8. Brinkert K, De Causmaecker S, Krieger-Liszkay A, Fantuzzi A, & Rutherford AW (2016) Bicarbonate-induced redox tuning in Photosystem II for regulation and protection. *Proc. Natl. Acad. Sci. USA* 113(43):12144-12149.
9. Glasoe PK & Long FA (1960) Use of glass electrodes to measure acidities in deuterium oxide. *J. Phys. Chem.* 64(1):188-190.
10. Zwietering MH, Jongenburger I, Rombouts FM, & van 't Riet K (1990) Modeling of the Bacterial Growth Curve. *Appl. Environ. Microbiol.* 56(6):1875-1881.
11. Zhang M*, et al.* (2017) Structural insights into the light-driven auto-assembly process of the water-oxidizing Mn_4CaO_5-cluster in photosystem II. *eLife* 6:e26933.
12. Luber S*, et al.* (2011) S_1-State Model of the O_2-Evolving Complex of Photosystem II. *Biochemistry* 50(29):6308-6311.
13. Kaur D*, et al.* (2019) Relative stability of the S_2 isomers of the oxygen evolving complex of photosystem II. *Photosyn. Res.*
14. Song Y, Mao J, & Gunner MR (2009) MCCE2: Improving protein pK_a calculations with extensive side chain rotamer sampling. *J. Comput. Chem.* 30(14):2231-2247.
15. Tannor DJ*, et al.* (1994) Accurate First Principles Calculation of Molecular Charge Distributions and Solvation Energies from Ab Initio Quantum Mechanics and Continuum Dielectric Theory. *J. Am. Chem. Soc.* 116(26):11875-11882.